Turkish Journal of Earth Sciences (Turkish J. Earth Sci.), Vol. 19, 2010, pp. 527–542. Copyright ©TÜBİTAK
doi:10.3906/yer-0905-1 First published online 22 October 2010

Ontogeny and Funtional Morphology of a Lower Cretaceous Carpinid Rudist (Bivalvia, Hippuritoida)

ROBERT W. SCOTT[1] & MEGHAN WEAVER[2]

[1] Precision Stratigraphy Associates and University of Tulsa, RR3 Box 103-3, Cleveland Oklahoma 74020, USA
(E-mail: rwscott@ix.netcom.com)

[2] Samson Resources Company, Two West Second Street, Tulsa Oklahoma 74103, USA

Received 3 May 2009; revised typescript received 24 June 2009; accepted 1 July 2009

Abstract: Caprinuloidea rudists are locally abundant and widespread in Lower Cretaceous (Albian Stage) Edwards Formation in Texas. Landward of the shelf margin on the shallow marine Comanche Shelf rudists built circular and elongate bioherms with coarse-grained flank deposits. Two caprinid morphotypes suggest that some lived as elevators above the substrate and others were recumbent upon mobile grain flats. Elevators have elongated attached valves and weakly coiled free valves and recumbents have arcuate attached valves and strongly coiled free valves.

Detailed morphologic studies are not possible on the many molds and casts, but a few specimens are silicified. Their internal structures can be seen by X-ray computed tomographic scanning (CT), which provides three-dimensional representations of internal features. This technique enables the specific identification of caprinid rudists that otherwise could only be identified by sectioning the specimen. The abundant Edwards species is identified as *Caprinuloidea perfecta* because it has only two rows of polygonal canals on its ventral and anterior margins. X-ray CT images reveal ontogenetic stages of these unusual gregarious bivalves. Allometric to isometric growth characterizes the left-free valve (LV). Although the prodissoconch is unknown, the plots suggest that the initial length was greater than the width, which is like the D-shaped prodissoconch of Cardiacea. The LV has the morphology of loosely coiled gastropods and the right-attached valves are elongated and are unlike most Bivalvia.

Key Words: Caprinid rudists, CT X-ray, functional morphology, Lower Cretaceous, ontogeny, Texas

Bir Alt Kretase Caprinid Rudistinin (Bivalvia, Hippuritoida) Ontojenezi ve Fonksiyonel Morfolojisi

Özet: Caprinuloidea rudistleri Texas'daki Erken Kretase (Albiyen Katı) yaşlı Edwards Formasyonu'nda lokal olarak bol ve yaygın şekilde bulunur. Rudistler, sığ denizel Comanche Şelf'inde şelf kenarının karaya doğru olan bölümünde, kaba taneli kanat tortulları ile birlikte dairesel ve uzunlamasına biyohermler oluşturmuştur. İki kaprinid morfotipi, bazı rudistlerin sert zemin üzerinde zemine dik olarak, bazı rudistlerin de kırıntılı ve hareketli zemin üzerinde kıvrık olarak yaşadıklarını göstermektedir. Dik olanlar, uzamış sabit kavkıya ve hafifçe sarılmış serbest kavkıya, kıvrık olanlar ise kıvrılmış sabit kavkıya ve ileri derecede sarılmış serbest kavkıya sahiptir.

Çok sayıdaki iç ve dış kalıpta ayrıntılı morfolojik çalışma mümkün değildir, ancak bazı örnekler silisleşmiştir. Bunların iç yapıları, iç özelliklerinin üç boyutlu izlenebildiği X ışınlı bilgisayarlı tomografi taramasıyla (CT) görülebilir. Bu teknik caprinid rudistlerin tür bazında tanımlanmasını mümkün kılar, aksi takdirde örneğin kesilerek tayin yapılması gerekir. Bol miktardaki Edwards örnekleri, örneklerin ventral ve anterior kenarlarında sadece iki sıra poligonal kanal içermesinden dolayı *Caprinuloidea perfecta* olarak tanımlanmıştır. X ışını CT görüntüleri, bu alışılmadık iri boyutlu bivalviaların ontojenik aşamalarını ortaya çıkarmaktadır. Allometrik-isometrik büyüme sol-serbest kavkıyı (LV) karakterize eder. Hernekadar prodisokonş bilinmese de, ilksel uzunluğun genişlikten daha fazla olduğunu gösterir ve bu yapı Cardiacea'nın D-şekilli prodiskonş'una benzer. LV gevşek sarılmış bir gastropodun morfolojisine sahiptir, uzamış sağ-sabit kavkı ise birçok bivalviada gözlenmeyen bir özellik sunar.

Anahtar Sözcükler: Caprinid rudistler, CT X ışını, fonksiyonel morfoloji, Alt Kretase, ontojeni, Teksas

Introduction

Rudists were aberrant marine sessile suspension feeding bivalves that, together with corals and sponges, were important organisms in shallow-water Cretaceous buildups (Scott 1981, 1990; Höfling & Scott 2002). The primitive Late Jurassic rudist shell was a pair of coiled valves with a thin aragonitic inner shell layer and a thicker outer calcite layer. Most Cretaceous rudists possessed a very inequivalved shell, in which the inner shell layer became very wide and the outer layer was much thinner. Rudists are common in the Albian Edwards Formation and its correlative units, which crop out in a narrow sinuous band from southeastern Oklahoma to West Texas (Figure 1). The updip units represent paralic and open shelf carbonate facies on the broad Comanche Shelf. Units correlative with the Edwards extend downdip into the subsurface to the shelf margin, slope and basin facies (Scott 1990; Scott *et al.* 2003). In central Texas this lithostratigraphic unit has served as a model of rudist associations and rudist hydrocarbon reservoirs (Nelson 1959).

Caprinid rudists are common in the upper part of the Edwards Formation, which spans from the middle Albian to the lower part of the upper Albian (Figure 2) (Amsbury 2003; Scott *et al.* 2003). These elongate shells tend to be inclined or horizontal to bedding and many have been broken. Sand-sized rudist debris is an abundant component of the sedimentary fabric (Frost 1967). The caprinids formed biostromes and low-relief, elongate to ovate bioherms on the inner shelf (Roberson 1972; Scott 1990; Amsbury 2003). Although caprinids are locally abundant in the Edwards Formation in Texas, few specimens preserve the internal morphological features that enable species identification. Most caprinid specimens from the Edwards Formation are recrystallized or even partially dissolved and replaced by secondary calcite. Many specimens are internal molds that preserve no diagnostic morphologic features. Consequently study of phylogeny, ontogeny, and functional morphology has been impeded. Four species are documented from this stratigraphic interval (Scott 2002; Scott & Filkorn 2007): *Caprinuloidea perfecta* Palmer 1928, *Caprinuloidea multitubifera* Palmer 1928, *Texicaprina orbiculata* (Palmer 1928), and *Texicaprina vivari* (Palmer 1928).

However, recent examination of one caprinid specimen by X-ray Computed Tomography (CT) scanning shows the general outlines of the specimen and successive slices can be stacked by computer to form 3-D images (Molineux & Triche 2007; Molineux *et al.* 2007; images are on-line at http://digimorph.org/specimens/Caprinuloidea_perfecta/). The attenuated x-rays through carbonate cores are presented as colored images and reveal density patterns that relate to bulk density and lithology (Hughes *et al.* 2004). CT X-ray scanning reveals internal morphology of many organisms, for example echinoderms (Domínguez *et al.* 2002) among others.

Here we report on the ontogeny and functional morphology of silicified caprinid bivalves from the Lower Cretaceous (Albian Stage, middle to lower upper substages) Edwards Formation, Travis County, Texas. X-ray Computed Tomography (CT) scanning technique enables the taxonomic identification of silicified caprinid rudists that otherwise could only be identified by sectioning the specimen (Molineux *et al.* 2010). Furthermore, this technique provides a full three-dimensional representation that can be inspected from many positions so that a variety of internal features can be seen and measured enabling analysis of growth stages. Ontogenetic studies of rudists are just beginning (Steuber *et al.* 1998; Steuber 1999, 2000; Cestari 2005; Regidor-Higuera *et al.* 2007). For example the Late Cretaceous *Hippuritella vasseuri* (Douvillé) achieved maturity within 10 mm height as growth became cylindrical and the cardinal apparatus was developed (Götz 2003, 2007).

Material and Methods

Four well-preserved specimens from the Edwards Formation in Travis County are deposited in the Non-vertebrate Paleontology Laboratory (NPL) of the Texas Natural Science Center at The University of Texas at Austin. These were examined by CT scanning in order to identify internal structures (Appendix 1). One disarticulated RV-AV, TMM NPL4387, is well preserved and illustrates diagnostic internal structures. Other specimens are left valves.

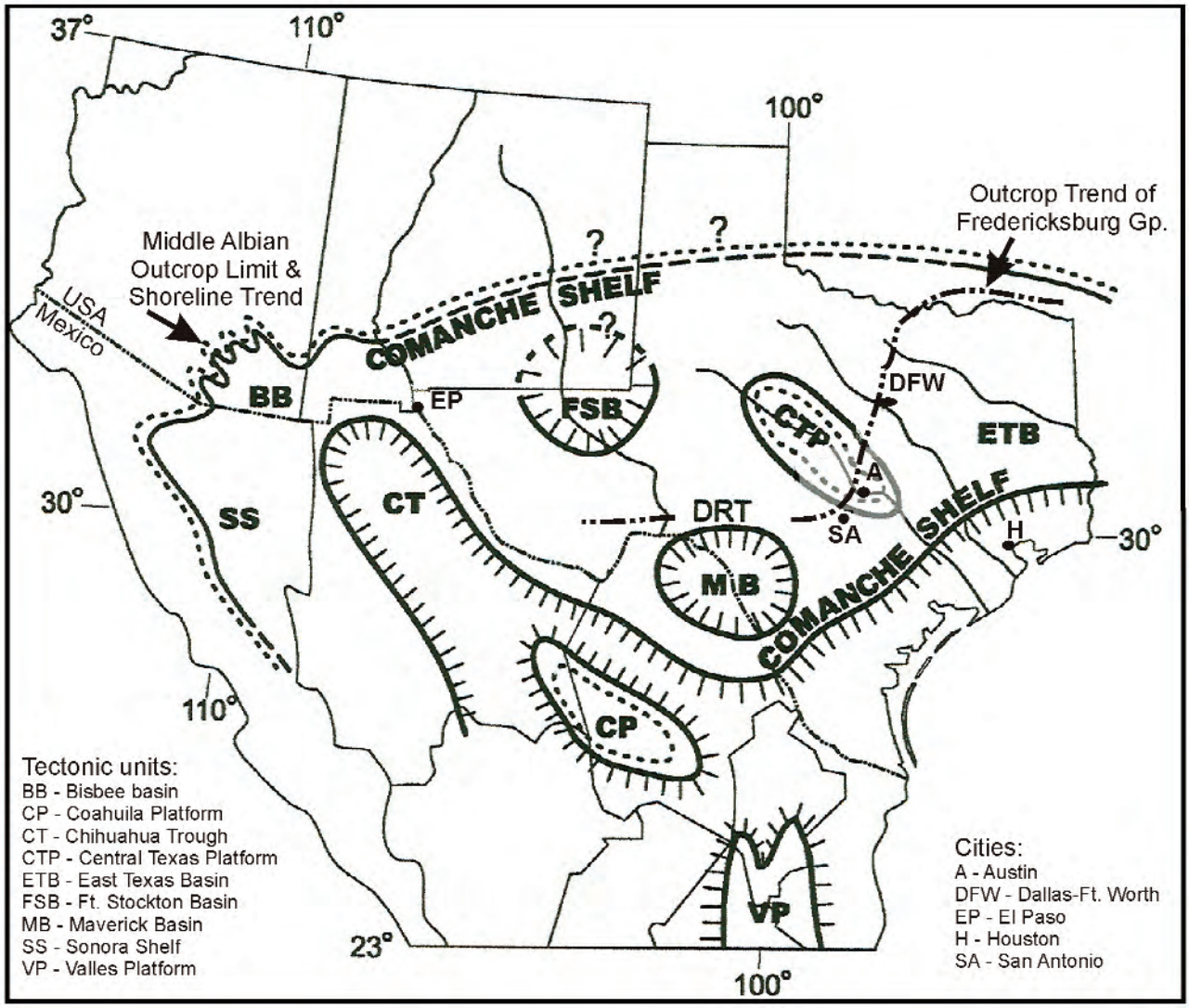

Figure 1. Middle Albian palaeogeographic map showing approximate outcrop trend of the Fredericksburg Group (adapted from Scott *et al.* 2003). Studied caprinid specimens were collected near Austin, Travis County, Texas.

High-resolution X-ray CT is a non-destructive technique for visualizing structures in the interior of opaque objects that enables palaeontologists to acquire digital information about the 3-D structural geometry of specimens. Its ability to resolve details as fine as a few tens of microns in objects made of high density material distinguishes this technique from traditional medical CAT-scanning. Complete details of the technique have been published and are available on-line (Ketcham & Carlson 2001; http://www.ctlab.geo.utexas.edu/overview/index.php#anchor2-2).

No specimen preparation is required prior to scanning, other than the need for the specimen to fit in the field of view. Because the full scan field is a cylinder, the most efficient geometry to scan is a cylinder. Commonly specimens are placed inside a cylindrical container with appropriate filler. This technique in many cases cannot be used successfully if the specimen and enclosing matrix have similar densities. The rudist specimens scanned here are silicified and the matrix is carbonate mud, providing an excellent contrast.

Scanning was done by Richard Ketcham in June 2007 at the University of Texas High-Resolution X-ray CT Facility. The specimens were first scanned with the high-energy 420-kV scanner subsystem in longitudinal direction to test for the presence of differentiable details. Following this successful test, the specimens were scanned perpendicular to the long axis using the microfocal subsystem with X-rays set at 180 kV and 0.133 mA to provide a focal spot of 30 µm. A total of 930 1024x1024 slices were obtained with a slice thickness and inter-slice spacing of 0.1433 mm and a field of reconstruction of 66 mm. Image processing and visualization was done by Jessie Maisano. The scan can be examined on the Digimorph site, an NSF Digital library at The University of Texas at Austin, http://digimorph.org/specimens/Caprinuloidea_ perfecta/.

Distribution and Morphology of *Caprinuloidea perfecta* Palmer 1928

The Family Caprinidae d'Orbigny (1847) [Order Hippuritoida Newell (1965), Superfamily Hippuritoidea Gray (1848)] was one of the most abundant and diverse Early Cretaceous rudist families. Within the Caprinidae clade the attached RV became elongated and the unattached valve became loosely coiled to cap-shaped. Uncoiling enabled uniform shell accretion along the entire mantle margin and the growth of conical forms (Skelton 1978). The family is divided into two subfamilies, Caprininae d'Orbigny (1847) and Caprinuloidinae Mac Gillavry (1970), which is the senior synonym of Coalcomaninae Coogan (1973). These two taxa are differentiated by the cardinal apparatus, ligament, posterior accessory cavity, pallial canals, and the protrusion of the posterior myophoral plate (Figure 3A, B) (Skelton & Masse 1998; Skelton & Smith 2000). The posterior myophore is a plate on either the left-free valve (LV-FV) or the right-attached (RV-AV) that projects down into a cavity of the opposing valve (Chartrousse 1998, figure 5.1). The anterior myophore is an inclined surface that may extend as a lamina across the commissure. In Caprininae the posterior myophore projects up from the RV-AV and in the Capinuloidinae it projects down from the LV-FV (Chartrousse 1998). However, in 2-D cross sections, as seen in many outcrop and core specimens, these features cannot be recognized. Thus 3-D views provided by CT images of well-preserved specimens are essential for taxonomic diagnosis.

Caprinuloidea Palmer (1928), a genus of the Subfamily Caprinuloidinae Mac Gillavry (1970), occurs in Albian rocks in Mexico, Southwestern USA and the Caribbean (Alencáster *et al.* 1999; Coogan 1973; Scott 2002; Payne *et al.* 2004). This genus has two teeth in the left-free valve (LV-FV) and one tooth in the right-attached valve (RV-AV). The body cavity is larger than the accessory cavity. Pallial canals surround much of the exterior valve margin. The ligament groove is external and is expressed interiorly as a ligament ridge. The muscle attachment sites (myophores) are on the interior margins of the valve (Skelton & Masse 1998). The two valves are highly unequal in size and have quite different shapes. The RV-AV is long and curved with a slight rotational twist. The LV-FV is trochospirally coiled with one or more whorls. The cross-sections of both valves are approximately quadrilateral.

Two species of *Caprinuloidea* are recognized in the Caribbean Province and the Gulf Coast: *C. perfecta* Palmer (1928) and *C. multitubifera* Palmer (1928) (Scott 2002). Both species range from lowermost Albian to the basal part of the Upper Albian (Figure 2) (Scott & Filkorn 2007). The two species are differentiated by the number of rows of polygonal canals; *C. perfecta* has two rows on its ventral and anterior margins and *C. multitubifera* has four or more (Coogan 1977) (Figure 3A, B).

The shell structure includes ventrally trifurcating marginal plates cut by radial plates to form two rows of polygonal canals (Figure 3A, B). The body cavity is slightly off center, with anterior and posterior tooth sockets separated by the central tooth and ligament ridge on the dorsal side. The ventral side is the thinnest of the skeleton and the anterior side is flattened to slightly concave; perhaps the anterior margin was recumbent upon the substrate. The ligament groove is external and attaches to the ligament ridge.

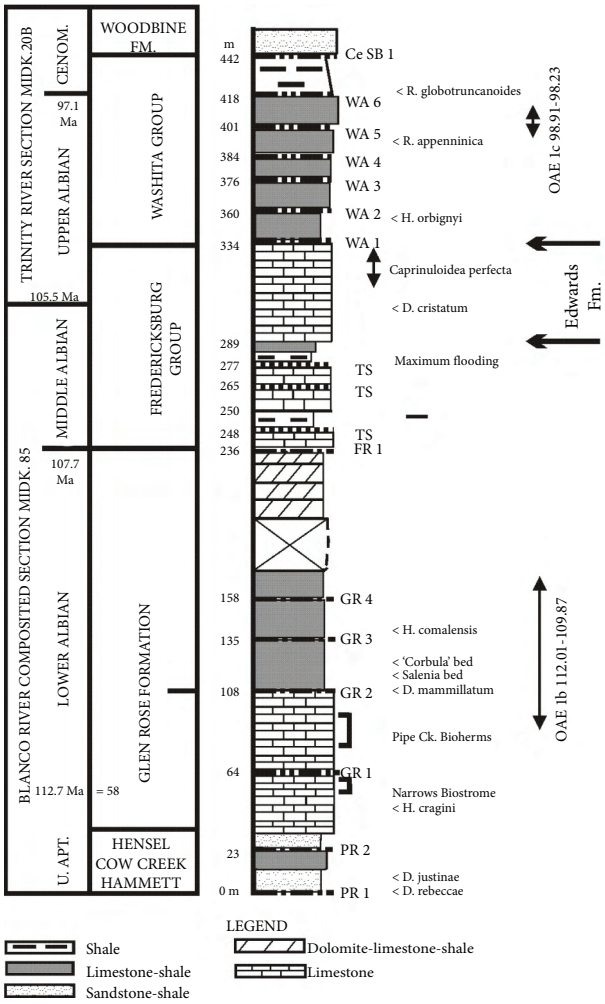

Figure 2. Composited Comanchean stratigraphy in central Texas (data from Scott *et al.* 2003; Mancini & Scott 2006; Ward & Ward 2007; González-León *et al.* 2008).

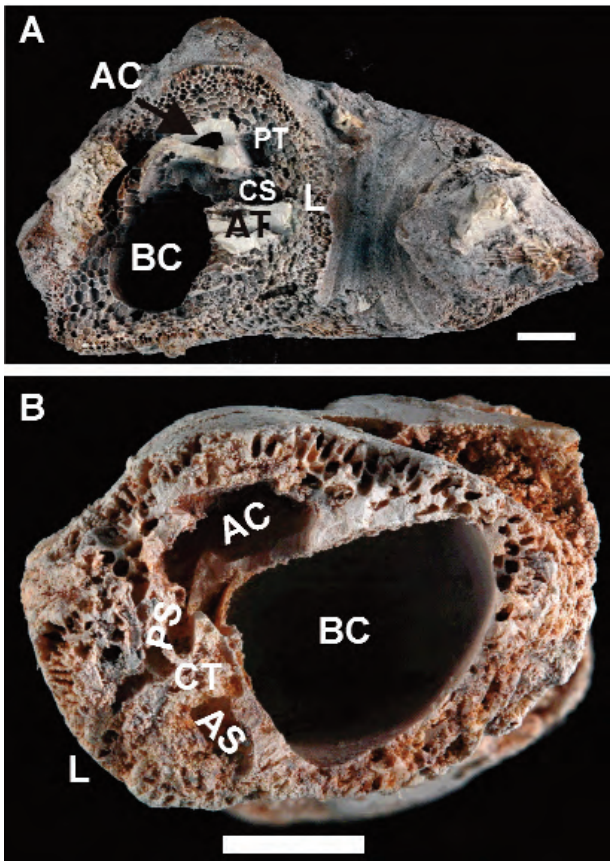

Figure 3. A. Morphological features of *Caprinuloidea perfecta* LV-FV NPL2381; B. RV-AV UT-11276. Scale bar= 1 cm. AC– accessory cavity; AT– anterior tooth; BC– body cavity; L– ligament. AS– anterior socket; PT– posterior tooth; PS– posterior socket; CT– central tooth; CS– central socket.

Ontogeny of *C. perfecta*

The size distribution of *C. perfecta* in in-situ assemblages relates to the mortality of the species. Observations of various assemblages in the Edwards Formation and related units suggest that most individuals grow to adult size and juvenile mortality is low. A collection of random silicified specimens in the collections of the Texas Natural Science Center consists mainly of LVs that are longer than 60 cm (Figure 4, Table 1). Collections from many single beds are needed to test the null hypothesis that juvenile mortality was high.

The growth pattern and growth rate were measured on three LVs (Table 2). Distinct widely spaced swellings indicate periodic growth that may represent annual cycles resulting from either climatic changes or reproductive activity (Figure 5). Eight to nine major growth rings were counted on three specimens. Between these coarse rings are 12 to 14 thinner growth rings. Our hypothesis is that the coarser rings record annual growth and the finer rings are monthly growth. The cumulative length from the valve apex to successive rings shows an early slow stage followed by an isometric stage (Figure 5). The complete growth cycle appears to

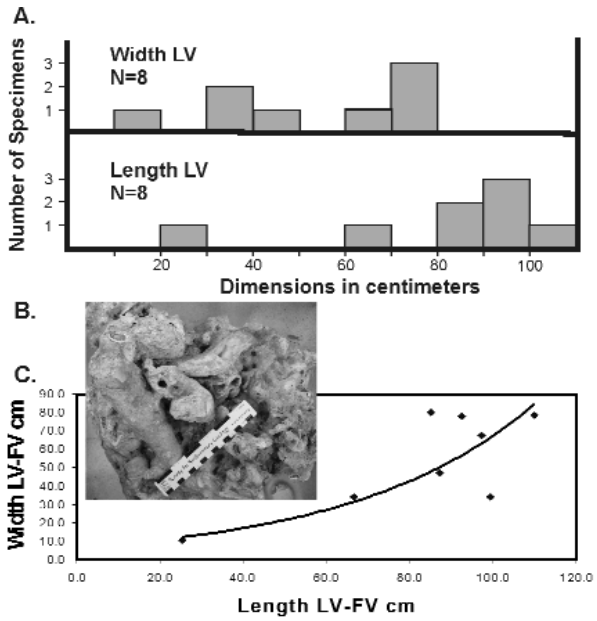

Figure 4. (A) Number of studied specimens in each size category. This is not a statistically representative sample from a specific bed. This distribution is consistent with field observations and suggests the hypothesis that many individuals of *C. perfecta* survived long. **(B)** Disturbed-neighborhood assemblage of *C. perfecta* showing mainly adult individuals. C. Plot of length to width of LVs in this study.

Table 1. Data for Figure 4A and C. NA– parameters could not be measured.

Specimen	Total Length (mm)	Dorsal-ventral Width (mm)
UT10932 RA	25.5	10.4
UT36137 RB	110.0	78.6
UT33864 RC	92.5	77.9
UT33800	97.3	67.5
NPL2381	87.1	47.1
UT33861	85.1	79.8
TX65-2B	102.0	NA
UT34818	66.7	34.0
UT11276L	99.5	34.1
NPL15739	230.0	NA
TX65-2A	180.0	NA

have been slightly allometric. This pattern is similar to the isometric growth of Early Cretaceous (Upper Albian) cardiids of the Western Interior seaway in Kansas (Scott 1978). If the coarse growth rings are annual, these specimens lived up to nine years or more. During this time interval some specimens grew to 268 to 305 mm in length, a rate of 22 to 25 mm/yr. This rate is faster than the rate of 6.9 mm/yr of *Kimbleia albrittoni* (Scott 2002) but within the 10 to 54 mm/yr range of Late Cretaceous hippuritids (Steuber 2000). Environmental factors may also produce growth rings. Growth rings in intertidal radiolitids were attributed to tidal rhythms by Regidor-Higuera *et al.* (2007).

The allometric to isometric growth pattern of the LV length is compared to the growth of the body cavity in the RV. The length and width of a well preserved RV increased allometrically during growth (Figure 6, Table 3). The growth rate of the body cavity was more rapid during the early stage than during the later stage when it decreased with age. During early growth the anterior-posterior and dorsal-ventral dimensions increased at about the same rate (Figure 6A). During the final stage the dorsal-ventral dimension increased more rapidly in this specimen. The body cavity area also increased more rapidly during early growth and decreased up to the final stage when it abruptly increased in this specimen (Figure 6B). The resulting growth pattern is allometric as the animal matured. The cyclic form of the curves (Figure 6A, C) resulted from measuring unbroken tabulae inserted periodically in the body cavity.

The virtual isometric growth of the LV and the decreasing allometric growth of the body cavity in the RV appear to be inconsistent. Although the valve length increased uniformly with age its body cavity growth rate decreased with age. Thus other internal valve structures must have increased. Clearly the accessory cavity increased in area with age; compare CT slices 150 through 1600 (Figure 6D). This differential rate should be tested by measurements. One hypothesis is that as the individual matures sexually more space is required for gamete production. This may have been one function of the accessory cavity. In comparison Late Cretaceous

Table 2. Data for Figure 5.

Coarse Growth Rings	Dorsal-ventral Diameter (mm)	Cumulative Diameter (mm)
UT10932 RA		
1	15.0	15.0
2	8.5	23.5
3	12.0	35.5
4	15.0	50.5
UT33864 RC		
4	41.5	41.5
5	33.5	75.0
6	31.2	106.2
7	22.3	128.5
8	24.8	153.3
9	27.0	180.3
10	23.2	203.5
11	34.5	238.0
12	30.2	268.2
UT36137 RB		
4	58.5	58.5
5	38.0	96.5
6	26.5	123.0
7	36.5	159.5
8	31.2	190.7
9	28.5	219.2
10	25.8	245.0
11	30.5	275.5
12	30.0	305.5

radiolitid species grew either isometrically or allometrically decreasing with age (Steuber *et al.* 1998, figure 14; Steuber 2000, figure 5), whereas ontogeny of the hippuritid, *Vaccinites chaperi*, was allometric (Steuber 1999).

A series of coronal slices of one RV from near the apex at an early growth stage to its commissure (Molineux *et al.* 2007) shows that the body cavity, accessory cavity and anterior tooth socket developed early and simply enlarged during growth (Figure 6D). The posterior pallial canals, however, were inserted at a stage about 1.5 cm from the apex. Although somewhat obscured by silicification, it appears that the pyriform pallial canals developed first and about 2 cm from the apex the polygonal canals began to appear. This insertion pattern suggests that pallial canals served a function beginning early and were not associated with maturity and reproduction.

Analysis of serial sections of left valves shows the order of insertion of internal structures. The interiors of two valves are preserved and the valves were scanned in parallel slices that initially were approximately normal to the commissure. Because the valves are torted the scans became oblique and some slices intersect both the late stage and early stage (Figures 7 & 8). The three-part pattern of body cavity, accessory cavity and socket were developed early in the ontogeny and grew larger but did not

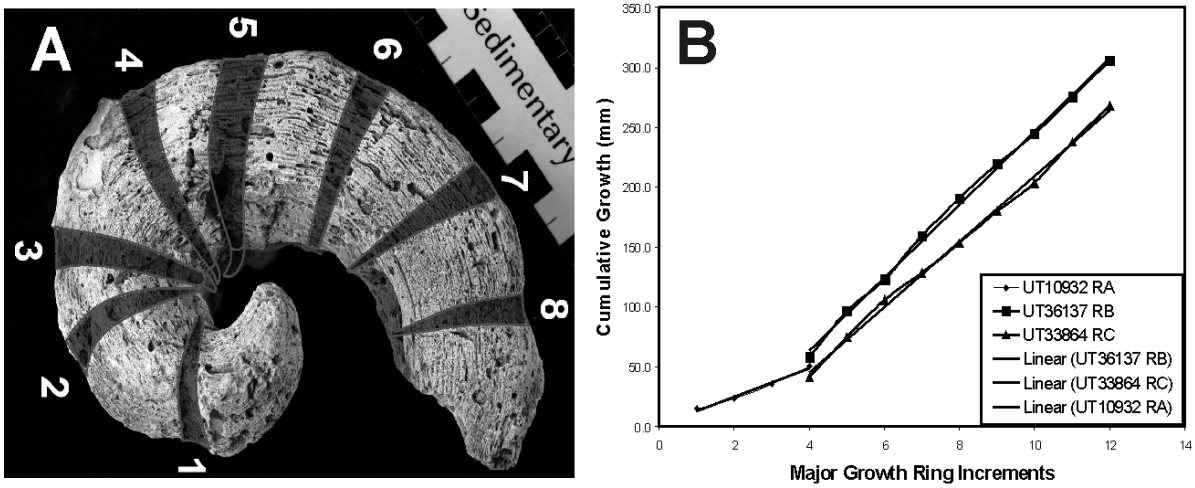

Figure 5. (A) Major growth rings of a LV of *C. perfecta* and **(B)** plot of cumulative growth rate of three LVs.

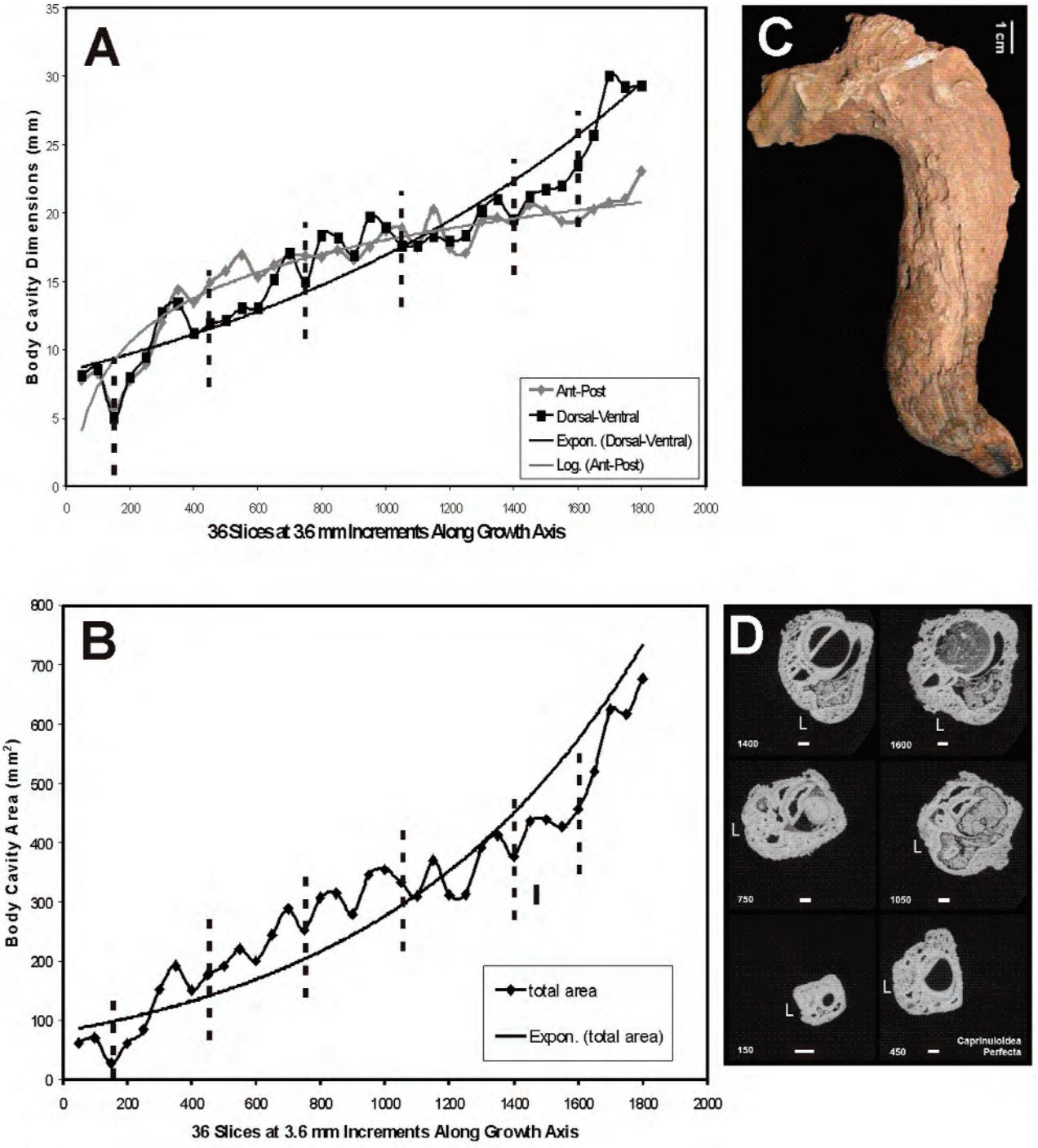

Figure 6. Growth form of *C. perfecta* (NPL4387: RV-AV) measured in anterior-posterior (diamond) and dorsal-ventral (square) dimensions **(A)**; **(B)** plot of body cavity area at successive growth increments; **(C)** lateral view of measured specimen; **(D)** serial sections of NPL4387. The logarithmic curve better fits the anterior-posterior growth and the exponential curve better fits the dorsal-ventral growth. L– ligament position.

Table 3. Data for Figure 6.

NPL4387: RV-AV			
Slice	Anterior-posterior mm	Dorsal-ventral mm	Total area mm^2
50	7.7382	8.09645	62.65194939
100	8.23975	8.598	70.8453705
150	5.66035	5.0155	28.38948543
200	7.7382	8.0248	62.09750736
250	8.95625	9.4578	84.70642125
300	11.96555	12.7537	152.605035
350	14.40165	13.39855	192.9612276
400	13.4702	11.24905	151.5269533
450	14.9032	11.8939	177.2571705
500	15.763	12.1805	192.0012215
550	16.9094	13.0403	220.5036488
600	15.3331	13.0403	199.9482239
650	16.1929	15.11815	244.8066911
700	16.9094	17.0527	288.3509254
750	16.83775	14.97485	252.1427806
800	16.7661	18.3424	307.5305126
850	17.26765	18.1991	314.2556891
900	16.55115	16.9094	279.8700158
950	17.55425	19.70375	345.8845534
1000	18.70065	18.98725	355.0739167
1050	18.9156	17.6259	333.404474
1100	17.55425	17.6259	309.4094551
1150	20.27695	18.27075	370.4750842
1200	17.41095	17.9125	311.8736419
1250	17.0527	18.3424	312.7874445
1300	19.41715	20.2053	392.3293409
1350	19.6321	20.99345	412.1455097
1400	19.27385	19.56045	377.0051792
1450	20.56355	21.2084	436.1199938
1500	20.2053	21.70995	438.6560527
1550	19.41715	21.99655	427.1103108
1600	19.41715	23.5012	456.3263256
1650	20.27695	25.6507	520.1179614
1700	20.7785	30.02135	623.798621
1750	21.0651	29.2332	615.8002813
1800	23.0713	29.30485	676.1009858

change shape or positions relative to each other (Figure 7). A pallial canal zone is present very near the apex of the LV and pallial canals were formed at an early growth stage (Figure 8).

Functional Morphology

Few specimens of *C. perfecta* are known in growth position. Indeterminate caprinid species in the Edwards Formation comprise circular to elongate bioherms and are oriented upright to inclined to horizontal (Roberson 1972). In bioclastic grainstone facies the caprinids are suparallel to the substrate (Scott 1990) either because of transport or because they lived in a recumbent position.

The RV-AV of *C. perfecta* is elongated and S-shaped (Figure 4B; specimen NPL4387), which is typical of a recumbent morphotype (Skelton & Gili 2002). However, the geniculate form of specimen NPL4387 suggests displacement during growth from an elevator to a recumbent position. The LV-FV is trochospirally coiled with translation toward the posterior so that from the anterior view the shell is coiled clockwise. The anterior margin is flat to slightly concave and the posterior margin abruptly rounded to keeled. This form would be adaptive to a recumbent position lying on the anterior side with the coil into the substrate. This position would maintain the commissure at or above the substrate and clear of sediment. This attitude is substantiated by the presence of epizoans on the posterior side of the LV (Figures 5 & 7). Siphonate bivalves are oriented with the posterior margin approximately normal to the substrate in order to intake and expel water. Although no morphologic structures of *Caprinuloidea* suggest the presence of siphons, the regular flow of seawater across their body was necessary to provide food, to clean the mantle of fecal matter and to expel gametes.

The 3-D molluscan valve configuration can be modeled from four dimensions: the shape of the generating curve, which is the commissural outline, the rate of whorl expansion, W, the increasing distance of the generating curve from the axis, D, and the translation along the coiling axis, T (Raup 1966; Raup & Stanley 1971). Valve measurements were derived from photographic images of four LV-FVs

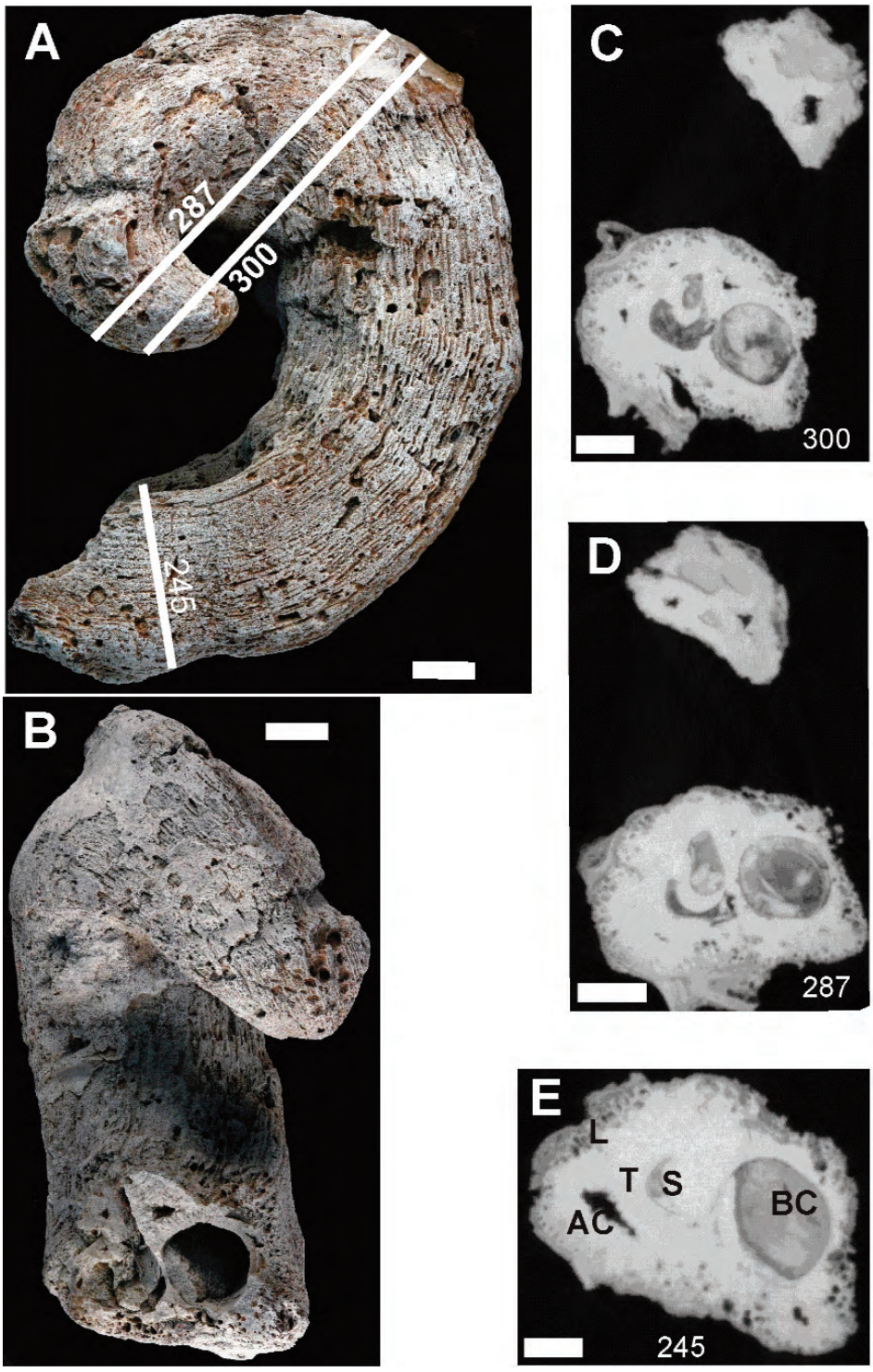

Figure 7. Adult *C. perfecta* LV, UT36137. **(A)** Anterior view. **(B)** Dorsal view of same specimen; note epizoans on posterior margin. **(C)** CT slice 300 through commissural and apical sections of whorl. **(D)** CT slice 287 through commissural and apical sections of whorl. **(E)** CT slice 245 parallel to commissure. AC– accessory cavity, BC– body cavity, L– ligament ridge, S– socket, T– tooth. Bar on all images– 1 centimeter.

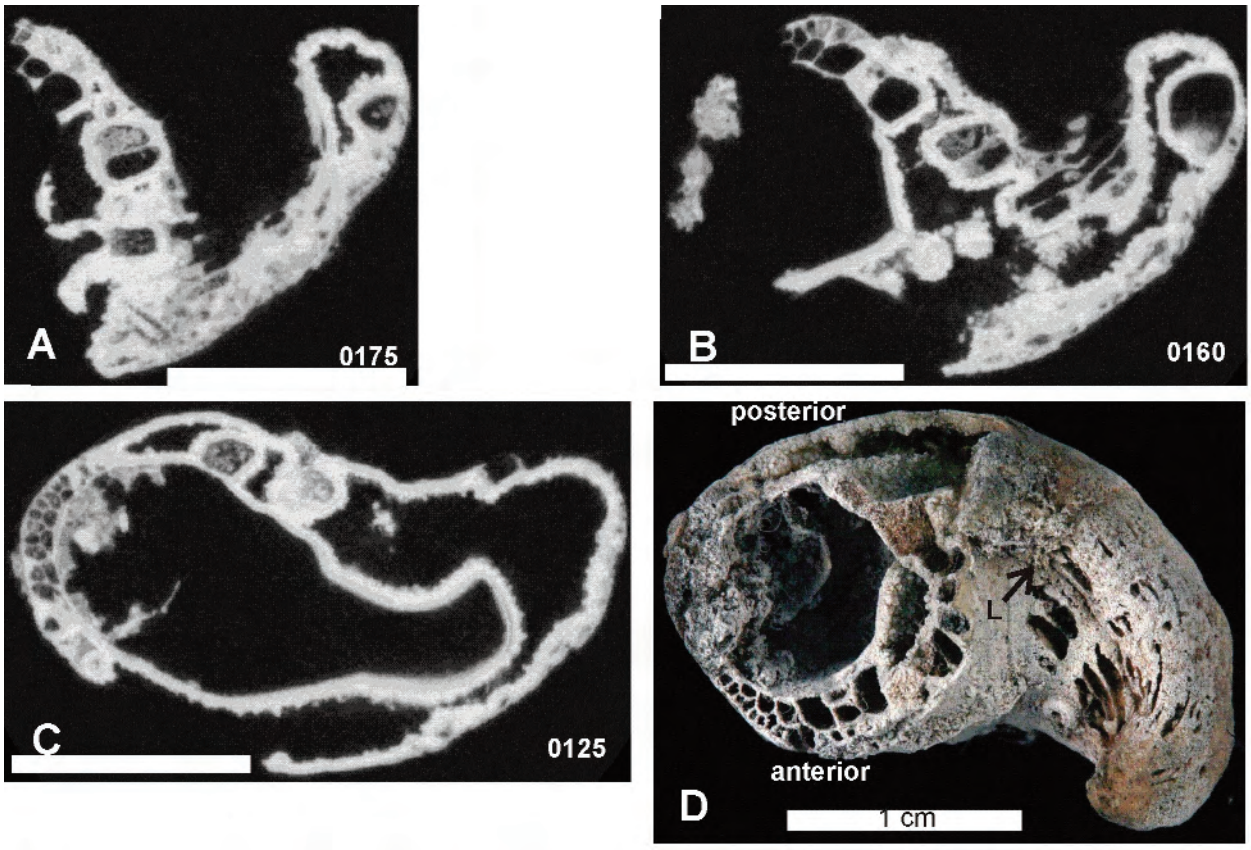

Figure 8. Juvenile *C. perfecta* LV, UT50222. **(A)** Oblique CT slice 0175 through apex and dorsal margin near commissure. **(B)** Oblique CT slice 0160 from apex to commissure. **(C)** Oblique CT slice 0125 through dorsal margin. **(D)** Dorsal view of same specimen; L– ligament groove. Bar on all images– 1 centimeter.

and one RV-AV (Table 4). The whorl expansion rate, W, is the ratio between the distance from the coiling axis to the dorsal valve margin at 360° of the spiral (Figure 9). This ratio measures tightness or looseness of the coiling and is greater than one. The distance of the generating curve from the axis, D, is the ratio between the distances of the generating curve from the axis at two positions 360° apart. It is less than one, and here we use the inverse equation of the same two distances as for W. The translation along the coiling axis, T, is the ratio between the distance of the generating curve at one whorl and the distance from the axis to the center of the generating curve at the advanced whorl.

The coiling shell parameters of the LV-FV of *Caprinuloidea perfecta* fall within the 'traditional' fields of gastropods (Figure 9, Table 4). As in many gastropods the *C. perfecta* coil is slightly trochospiral and the expansion rate-W and distance of the generating curve from the coiling axis-T are within the gastropod form (Figure 9). In contrast the cylindrical, torted RV-AV is quite unlike that of either gastropods or bivalves. The translation-T is greater than most bivalves and the distance of the generating curve from the coiling axis-D is well outside of bivalves and gastropods. This coiling style suggests that the LV-FV functioned differently than either the basic bivalve shell or the gastropods shell. In the recumbent position the LV-FV was anchored in the mobile sediment by its apex and free to move slightly. As the shell opened the apex glided up toward the sediment surface and as it closed the apex twisted into the sediment like a screw. The longer, stick-like RV-AV was less mobile than the FV

because of the greater surface area in contact with the sediment, thus greater friction. Possibly the juvenile shell was elevated; as the shell grew some toppled into a recumbent position and others remained elevated to inclined supported by neighboring shells. The gastropod-like form of the LV resulted from differential growth of the mantle of the two valves.

The LV of *C. perfecta* is comparable to the LV of *Kimbleia capacis* Coogan, 1973 in the Upper Albian Devils River Formation in West Texas (Scott & Kerans 2004). The LV of *K. capacis* is virtually a planispiral coil of one and a half whorls (Scott 2002, figure 4). Because its center of gravity was displaced from the RV growth axis, it would have been quite unstable in an elevated position; but in a recumbent attitude it would be quite stable and resistant to displacement by low energy currents. However the LV of *Kimbleia albrittoni* (Perkins 1961) was coiled less than a one-half whorl and was stable in the elevated position (Scott 2002, figure 5).

Conclusions

The application of high-resolution X-ray CT scanning has the capability to illustrate preserved internal morphological structures of rudists that otherwise could only be studied by destruction of the specimen (Domínguez *et al.* 2002; Molineux *et al.* 2007, 2010). Traditional sectioning by diamond saw requires that the angles and positions of cutting be predetermined. If serial sections are made the specimen is completely destroyed. CT X-ray scanning is non-destructive and specimens may be viewed from many different angles. The enhancement of scanned images may reveal structures that could not be observed in traditional sections. Detailed measurements of different structures are possible in 3-D images as thin as 0.1433 mm that cannot be made in thicker traditional serial sections. In addition CT images may reveal minute ontogenetic changes that may be lost in sawed sections.

This study of selected silicified specimens of *Caprinuloidea perfecta* from the Edwards Formation in central Texas illustrates the unique morphological data obtainable by CT scanning. Growth rate of these shells at about 25 mm per major growth ring was much faster than the upper Albian *Kimbleia albrittoni*, which has major growth rings about 6.9 mm apart (Scott 2002). In comparison growth rates of Late Cretaceous hippuritid rudists ranged from less than 10 to 54 mm (Steuber 2000). Serial sections show that the accessory cavity formed early in ontogeny but slightly later than the body cavity. Pallial canals were also early formed structures. Thus they were functional beginning in the early growth stage following larval settlement.

Functional morphology of *Caprinuloidea perfecta* is analyzed using the 3-D morphometric cube. The elongate, sinuous RV falls well outside of the fields of 'normal' bivalves and gastropods. However the LV shape is typical of many gastropods.

Table 4. Data for Figure 9.

UT Museum Specimen #	d_1 mm	d_2 mm	$D=d_1/d_2$	$W=d_2/d_1$	t mm	d_3 mm	$T= t/d_3$
UT36137	7.4	36	0.21	4.9	41.1	52.6	0.78
UT33864	2.8	18.3	0.15	6.5	31.1	38.9	0.8
UT33800	2.6	10.5	0.25	4	38.4	31.6	1.2
NPL2381	1.1	16.8	0.07	15.3	0	42.1	0
NPL4387			high	medial			high

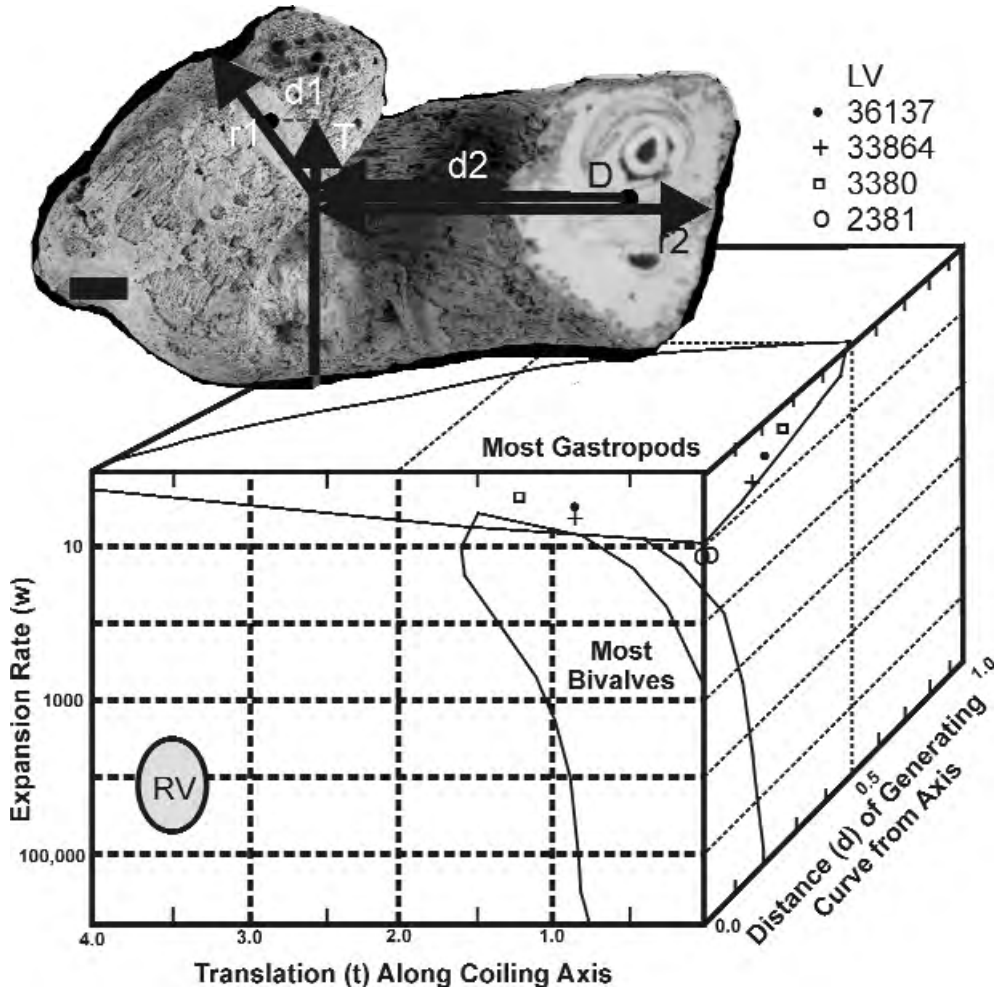

Figure 9. Three-D morphological plot of *C. perfecta* and dimensions measured.

Acknowledgements

Funding for scanning was provided to M. Weaver by the Graduate Research Office and Geosciences Department of the University of Tulsa, to Timothy Rowe of the Department of Geological Sciences, The University of Texas at Austin, by a National Science Foundation Digital Libraries Initiative grant IIS-0208675, and to R.A. Ketchum for support of the University of Texas High-Resolution X-ray CT Facility by NSF Grant EAR-0345710. Matthew Colbert scanned the specimens and Jessica Maisano processed the images at the X-ray CT Facility. Field work was supported by Ann Molineux of the University of Texas Austin, The University of Tulsa, and Precision Stratigraphy Associates.

References

Alencáster, G., Torres-Hernández, R., Tristan-González, M., Barbosa-Gudiño, R. & López-Doncel, R. 1999. El Abra Formation in the western part of the Valles-San Luis Potosí Platform (México). *In*: Höfling, R. & Steuber, T. (eds), *Fifth International Congress on Rudists – Abstracts and Field Trip Guides.* Erlanger geologische Abhandlungen **3**, 7–8.

Amsbury, D. 2003. Stratigraphy of Fredericksburg Group (Middle–Upper Albian Cretaceous) of North-Central Texas. *In:* Scott, R.W. (ed), *Cretaceous Stratigraphy and Paleoecology, Texas and Mexico.* Perkins Memorial Volume. Gulf Coast Section Society of Economic Paleontologists and Mineralogy Foundation, Special Publications **1**, 227–276.

Cestari, R. 2005. New data on the relationship between shape and palaeoenvironment in Late Cretaceous rudists from Central Italy. *Società Paleontologica Italiana, Bollettino* **44**, 185–192.

Chartrousse, A. 1998. The myocardinal organization of coalcomaninid rudists revisited. *In:* Masse, J.-P. & Skelton, P.W. (eds), *Quatrième Congrès International sur les Rudistes.* Geobios, Mémoire Spécial **22**, 75–85.

Coogan, A.H. 1973. New rudists from the Albian and Cenomanian of Mexico and south Texas. *Revista del Instituto mexicano del Petróleo* **5**, 1–83.

Coogan, A.H. 1977. Early and middle Cretaceous Hippuritacea (rudists) of the Gulf Coast. *In:* Bebout, D.G. & Loucks, R.G. (eds), *Cretaceous Carbonates of Texas and Mexico.* University of Texas at Austin, Bureau of Economic Geology, Report of Investigations **89**, 32–70.

D'Orbigny, A. 1847. Considérations zoologiques et géologiques sur les Brachiopodes ou Palliobranches. *Comptes Rendus Hebdomadaires des Séances de l'Académie des Sciences* **25**, 266–269.

Domínguez, P., Jacobson, A.G. & Jefferies, R.P.S. 2002. Paired gill slits in a fossil with a calcite skeleton. *Nature* **417**, 841–844.

Frost, J.G. 1967. Edwards Limestone of central Texas. *In:* Hendricks, L. (ed), *Comanchean (Lower Cretaceous) Stratigraphy and Paleontology of Texas.* The Permian Basin Section, Society of Economic Paleontologists and Mineralogists, Publication **67–8**, 133–156.

Gray, J.E. 1848. On the arrangement of the brachiopoda. *Annals and Magazine of Natural History* **2**, 435–440.

González-León, C.M., Scott, R.W., Löser, H., Lawton, T.F., Robert, E. & Valencia, V.A. 2008. Upper Aptian–Lower Albian Mural Formation: stratigraphy, biostratigraphy and depositional cycles on the Sonoran Shelf, northern México. *Cretaceous Research* **29**, 249–266.

Götz, S. 2003. Larval settlemment and ontogenetic development of *Hippuritella vasseuri* (Douvillé) (Hippuritoidea, Bivalvia). *Geologica Croatia* **56**, 123–131.

Götz, S. 2007. Inside rudist ecosystems: growth, reproduction, and population dynamics. *In:* Scott, R.W. (ed), *Cretaceous Rudists and Carbonate Platforms: Environmental Feedback.* SEPM (Society for Sedimentary Geology), Special Publications **87**, 97–113.

Höfling, R. & Scott, R.W. 2002. Early and mid-Cretaceous buildups. *In:* Kiessling, W., Flügel, E. & Golonka, J. (eds), *Phanerozoic Reef Patterns.* SEPM (Society for Sedimentary Geology) Special Publication **72**, 521–548.

Hughes, G.W., Siddiqui, S. & Sadler, R.K. 2004. Computerized tomography reveals Aptian rudist species and taphonomy. *Geologica Croatica* **57**, 67–71.

Ketcham, R.A. & Carlson, W.D. 2001. Acquisition, optimization and interpretation of X-ray computed tomographic imagery. *Applications to the Geosciences: Computers and Geosciences* **27**, 381–400.

Mac Gillavry, H.J. 1970. Geological history of the Caribbean, 1. *Koninklijke Akademie van Wetenschappen, Proceedings* **B73 (1)**, 64–83.

Mancini, E.A. & Scott, R.W. 2006. Sequence stratigraphy of Comanchean Cretaceous outcrop strata of northeast and south central Texas: implications for enhanced petroleum exploration. *Gulf Coast Association of Geological Societies Transactions* **56**, 539–550.

Molineux, A. & Triche, N. 2007. Rudist collections as a research resource at the Texas Natural Science Center. *In:* Scott, R.W. (ed), *Cretaceous Rudists and Carbonate Platforms: Environmental Feedback.* SEPM (Society for Sedimentary Geology), Special Publication **87**, 231–236.

Molineux, A., Scott, R.W., Ketcham, R.A. & Maisano, J. 2007. Rudist taxonomy using high-resolution X-ray Computerized tomography. *Paleontologica Electronica* **10(3)**, 13A, 6 p; http://palaeo-electronica.org/2007_3/135/index.html.

Molineux, A., Scott, R.W., Maisano, J., Ketcham, R. & Zachos, L. 2010. Blending rudists with technology: non-destructive examination internal and external structures using high quality scanning and digital imagery. *Turkish Journal of Earth Sciences* **19**, 757–767.

Nelson, H. 1959. Deposition and alteration of the Edwards Limestone, central Texas. *University of Texas Austin, Bureau of Economic Geology, Publication* **5905**, 21–96.

Newell, N.D. 1965. Classification of the Bivalvia. *American Museum of Natural History. Novitates* **2206**, 1–65.

Palmer, R.H. 1928. The rudistids of southern Mexico. *Occasional Papers of the California Academy of Sciences* **14**, 1–137.

Payne, J.L, Johnson, M.E. & Ledesma-Vazquez, J. 2004. Lower Cretaceous Alisitos Formation at Punta San Isidro. *Coastal Sedimentation and Volcanism. Ciencias Marinas* **30**, 365–380.

Perkins, B.F. 1961. *Biostratigraphic Studies in the Comanche (Cretaceous) Series of Northern Mexico and Texas*. Geological Society of America Memoir **83**.

Raup, D.R. 1966. Geometric analysis of shell coiling: general problems. *Journal of Paleontology* **40**, 1178–1190.

Raup, D. & Stanley, S.M. 1971. *Principles of Paleontology*. W.H. Freeman and Company, San Francisco.

Regidor-Higuera, I., Garcia-Garmilla, F. & Skelton, P.W. 2007. Sclerochronology and diagenesis of Late Cretaceous radiolitids (Bivalvia, Hippuritoidea), Spain. *In:* Scott, R.W. (ed), *Cretaceous Rudists and Carbonate Platforms: Environmental Feedback.* SEPM (Society for Sedimentary Geology) Special Publication **87**, 115–139.

Roberson, D.S. 1972. The paleoecology, distribution and significance of circular bioherms in the Edwards Limestone of central Texas. *Baylor Geological Studies, Bulletin* **23**, 1–35.

Scott, R.W. 1978. Paleobiology of Comanchean (Cretaceous) cardiids (Cardiinae), North America. *Journal of Paleontology* **52**, 881–903.

Scott, R.W. 1981. Biotic relations in early cretaceous coral-algal-rudist reefs, Arizona. *Journal of Paleontology* **55**, 463–478.

Scott, R.W. 1990. Models and stratigraphy of mid-Cretaceous reef communities, Gulf of Mexico. *SEPM (Society for Sedimentary Geology), Concepts in Sedimentology and Paleontology* **2**, 1–102.

Scott, R.W. 2002. Albian caprinid rudists from Texas re-evaluated. *Journal of Paleontology* **76**, 408–423.

Scott, R.W., Benson, D.G., Morin, R.W., Shaffer, B.L. & Oboh-Ikuenobe, F.E. 2003. Integrated Albian–Lower Cenomanian chronostratigraphy standard, Trinity River section, Texas. *In*: Scott, R.W. (ed), *Cretaceous Stratigraphy and Paleoecology, Texas and Mexico.* Perkins Memorial Volume, GCSSEPM Foundation, Special Publications in Geology **1**, CD Book, 277–334.

Scott, R.W. & Filkorn, H.F. 2007. Barremian–Albian rudist zones, U.S. Gulf Coast. *In:* Scott, R.W. (ed), *Cretaceous Rudists and Carbonate Platforms: Environmental Feedback.* SEPM (Society for Sedimentary Geology) Special Publication **87**, 167–180.

Scott, R.W. & Kerans, C. 2004. Late Albian carbonate platform chronostratigraphy, Devils River Formation cycles, west Texas. *Courier Forschungsinstitut Senckenberg* **247**, 129–148.

Skelton, P.W. 1978. The evolution of functional design in rudists (Hippuritacea) and it staxonomic implications. *Philosophical Transactions of the Royal Society of London, Series* **B 284**, 305–318.

Skelton, P.W. & Gili, E. 2002. Palaeocological classification of rudist morphotypes. *In:* Sladić-Trifunović, M. (ed), *Rudists Proceedings – 1st International Conference on Rudists – Beograd, 1988.* Union of Geological Societies of Yugoslavia, Memorial Publication, 265–285.

Skelton, P.W. & Masse, J.-P. 1998. Revision of the Lower Cretaceous rudist genera *Pachytraga* Paquier and *Retha* Cox (Bivalvia: Hippuritacea), and the origins of the Caprinidae. *In :* Masse, J.-P. & Skelton, P.W. (eds), *Quatrieme Congres International sur les Rudistes.* Geobios Mémoire Spécial **22**, 331–370.

Skelton, P.W. & Smith, A.B. 2000. A preliminary phylogeny for rudist bivalves: sifting clades from grades. *In:* Harper, E.M., Taylor, J.D. & Crame, J.A. (eds), *The Evolutionary Biology of the Bivalves.* Geological Society, London, Special Publications **177**, 97–127.

Steuber, T. 1999. Cretceous rudists of Boeotia, central Greece. *Palaeontological Association, Special Papers in Palaeontology* **61**, 1–229.

Steuber, T. 2000. Skeletal growth rates of Upper Cretaceous rudist bivalves: implications for carbonate production and organism-environment feedbacks. *In:* Insalaco, E., Skelton, P.W. & Palmer, T.J. (eds), *Carbonate Platform Systems: Components and Interactions*. Geological Society, London, Special Publications **178**, 21–32.

Steuber, T., Yilmaz, C. & Löser, H. 1998. Growth rates of Early Campanian rudists in a siliciclastic-calcareous setting (Pontides Mts., North-Central Turkey). *Geobios, Mémoire spécial* **22**, 385–401.

Ward, W.C. & Ward, W.B. 2007. Stratigraphy of middle part of Glen Rose Formation (Lower Albian), Canyon Lake Gorge, Central Texas, U.S.A. *In:* Scott, R.W. (ed), *Cretaceous Rudists and Carbonate Platforms: Environmental Feedback.* SEPM (Society for Sedimentary Geology), Special Publications **87**, 191–210.

Appendix 1

Scanning and Processing data. Specimen scanned by Matthew Colbert, 27 June 2007. Ring-removal processing done by Jessie Maisano. Saved as 8-bit JPG and 16bit: 1024x1024 16-bit TIFF images.

Caprinid rudA: UT 10932. II, 180 kV, 0.13 mA, intensity control on, no filter, air wedge, no offset, slice thickness 2 lines (= 0.06389 mm), S.O.D. 92 mm, 1000 views, 2 samples per view, inter-slice spacing 2 lines (= 0.06389 mm), field of reconstruction 28 mm (maximum field of view 30.5046 mm), reconstruction offset 5300, reconstruction scale 5200. Acquired with 19 slices per rotation and 15 slices per set. Ring-removal processing based on correction of raw sinogram data using IDL routine 'RK_SinoRingProcSimul' with default parameters. Deleted first four duplicate slices of each rotation. Rotation correction processing done using IDL routine "DoRotationCorrection." Added back slices 2-4 and deleted last 12 blank slices. Total final slices = 216.

Caprinid rudB: UT 36137. II, 180 kV, 0.15 mA, intensity control on, no filter, empty container wedge, no offset, slice thickness 2 lines (= 0.2083 mm), S.O.D. 300 mm, 1000 views, 2 samples per view, inter-slice spacing 2 lines (= 0.2083 mm), field of reconstruction 92 mm (maximum field of view 99.47173 mm), reconstruction offset 4100, reconstruction scale 5300. Acquired with 19 slices per rotation and 15 slices per set. Flash- and ring-removal processing based on correction of raw sinogram data using IDL routines 'RK_SinoDeSpike' and 'RK_SinoRingProcSimul,' both with default parameters. Reconstructed with beam hardening coefficients [0, 0.75, 0.2]. Deleted first four duplicate slices of each rotation. Rotation correction processing done using IDL routine 'DoRotationCorrection.' Added back slices 2-4. Total final slices = 528.

Caprinid rudC: UT 33864; Gunn Ranch, NE of North San Gabriel, Williamson County, TX. II, 180 kV, 0.15 mA, intensity control on, no filter, empty container wedge, no offset, slice thickness 2 lines (= 0.2083 mm), S.O.D. 300 mm, 1000 views, 2 samples per view, inter-slice spacing 2 lines (= 0.2083 mm), field of reconstruction 92 mm (maximum field of view 99.47173 mm), reconstruction offset 4100, reconstruction scale 5300. Acquired with 19 slices per rotation and 15 slices per set. Ring-removal processing based on correction of raw sinogram data using IDL routine 'RK_SinoRingProcSimul' with default parameters. Reconstructed with beam hardening coefficients [0, 0.75, 0.2]. Deleted first four duplicate slices of each rotation. Rotation correction processing done using IDL routine "DoRotationCorrection." Total final slices = 450.

Caprinid rudis: UT33861, 36137, 10932, 33864, 8623, 11276, 24818, 33800, and NPL 2381. P250D, 419 kV, 1.8 mA, 1 brass filter, air wedge, no offset, 64 ms integration time, slice thickness = 0.5 mm, S.O.D. 673 mm, 1000 views, 1 ray averaged per view, 1 sample per view, inter-slice spacing = 0.5 mm, field of reconstruction 256 mm (maximum field of view 269.5545 mm), reconstruction offset 8500, reconstruction scale 6500. Total slices = 135.